

**Effect of isothermal ageing on the microstructure, shear behaviour and hardness of the Sn58Bi/SnAgCuBiNi/Cu solder joints**

Chang, Jian; Liu, Yang; Zhang, Hao; Zhou, Min; Yuxiong, Xue; Zeng, Xianghua; Cao, Rongxing; Chen, Penghui

**DOI**

[10.1080/09507116.2021.1889291](https://doi.org/10.1080/09507116.2021.1889291)

**Publication date**

2021

**Document Version**

Final published version

**Published in**

Welding International

**Citation (APA)**

Chang, J., Liu, Y., Zhang, H., Zhou, M., Yuxiong, X., Zeng, X., Cao, R., & Chen, P. (2021). Effect of isothermal ageing on the microstructure, shear behaviour and hardness of the Sn58Bi/SnAgCuBiNi/Cu solder joints. *Welding International*, 35(1-3), 3-11. <https://doi.org/10.1080/09507116.2021.1889291>

**Important note**

To cite this publication, please use the final published version (if applicable).  
Please check the document version above.

**Copyright**

Other than for strictly personal use, it is not permitted to download, forward or distribute the text or part of it, without the consent of the author(s) and/or copyright holder(s), unless the work is under an open content license such as Creative Commons.

**Takedown policy**

Please contact us and provide details if you believe this document breaches copyrights.  
We will remove access to the work immediately and investigate your claim.

ISSN: (Print) (Online) Journal homepage: <https://www.tandfonline.com/loi/twld20>

## Effect of isothermal ageing on the microstructure, shear behaviour and hardness of the Sn58Bi/SnAgCuBiNi/Cu solder joints

Jian Chang, Yang Liu, Hao Zhang, Min Zhou, Xue Yuxiong, Xianghua Zeng, Rongxing Cao & Penghui Chen

To cite this article: Jian Chang, Yang Liu, Hao Zhang, Min Zhou, Xue Yuxiong, Xianghua Zeng, Rongxing Cao & Penghui Chen (2021) Effect of isothermal ageing on the microstructure, shear behaviour and hardness of the Sn58Bi/SnAgCuBiNi/Cu solder joints, *Welding International*, 35:1-3, 3-11, DOI: [10.1080/09507116.2021.1889291](https://doi.org/10.1080/09507116.2021.1889291)

To link to this article: <https://doi.org/10.1080/09507116.2021.1889291>



Published online: 03 Mar 2021.



Submit your article to this journal [↗](#)



Article views: 82



View related articles [↗](#)



View Crossmark data [↗](#)

RESEARCH ARTICLE



## Effect of isothermal ageing on the microstructure, shear behaviour and hardness of the Sn58Bi/SnAgCuBiNi/Cu solder joints

Jian Chang<sup>a,b</sup>, Yang Liu<sup>b</sup>, Hao Zhang<sup>c</sup>, Min Zhou<sup>b</sup>, Xue Yuxiong<sup>b</sup>, Xianghua Zeng<sup>b</sup>, Rongxing Cao<sup>b</sup> and Penghui Chen<sup>b</sup>

<sup>a</sup>School of Material Science and Engineering, Harbin University of Science and Technology, Harbin, China; <sup>b</sup>College of Electrical, Energy and Power Engineering, Yangzhou University, Yangzhou, China; <sup>c</sup>Department of Microelectronics, Delft University of Technology, Delft, The Netherlands

### ABSTRACT

The microstructure, shear behaviour and hardness of the SnBi/SACBN/Cu solder joint before and after isothermal ageing were investigated in comparison with the SnBi/Cu and SACBN/Cu solder joints. The experimental results indicated that the pre-soldered SACBN joint had a significant effect on the formation and growth of the  $\beta$ -Sn grains in the SnBi bulk solder. The brittleness of the SnBi/SACBN/Cu composite solder joint was also suppressed and its failure mode transformed from brittle failure to brittle-ductile failure after reflow. However, the shear strength and failure mode of the SnBi/SACBN/Cu composite solder joint became similar to those of the SnBi/Cu joints after 600 h isothermal ageing. The shear strength of the three kinds of solder joints decreased after isothermal ageing, but the SnBi/SACBN/Cu composite solder joint showed higher shear strength than SnBi/Cu did during ageing. The shear strength of the composite solder joint was 67.1 MPa after ageing. Due to the diffusion of elements in the isothermal ageing process, the microstructure of the composite solder joint was significantly coarsened after ageing for 600 hours. This phenomenon further led to the decrease of the hardness and shear strength of the three kinds of solder joints.

### ARTICLE HISTORY

Received 16 December 2020  
Accepted 9 February 2021

### KEYWORDS

SnBi; SnAgCuBiNi; isothermal ageing; microstructure; shear behaviour; hardness

## 1. Introduction

Nowadays, with the increasing awareness of environmental protection, the traditional Sn-Pb solder has been replaced by lead-free solders. Among these, the Sn58Bi (SnBi) solder is widely used in the electronic packaging industry due to its low cost, low melting temperature of 139°C, good tensile strength and creep resistance [1–4]. However, the inherent brittleness of Bi element results in the insufficient ductility of Sn58Bi solder, which leads to a high risk of brittle fracture of the SnBi solder joint under mechanical shock or drop conditions. Therefore, it is of great importance to reduce the hardness and brittleness of the SnBi solder joints in order to broaden its further industrial applications.

One of the common methods to improve the performance of the SnBi solder joints is to add trace elements into the solder. Cheng et al. [5] found that adding 10% Ni to SnBi alloy reduced the thickness of IMC. In addition, the tensile strength of solder joints increased with the decrease of IMC thickness. Zhou et al. [6] studied the effects of Ti addition on the properties of SnBi alloys. The results showed that the microstructure of SnBi solder was refined after adding Ti. Adding 0.5 wt%

Ti after ageing achieved the highest yield strength and ultimate tensile strength. Sun et al. [7] analysed the mechanical properties of the SnBi solder joint doped with various amounts of carbon nanotubes (CNTs). The highest shear strength of 77.3 MPa was realized after adding 0.05 wt% CNTs. However, the shear strength of the SnBi solder joint decreased sharply when the doping amount overpassed 0.1 wt%. Ma et al. [8] found that the coarsening of Bi-rich phase and the growth of IMC in the SnBi/Cu solder joints were inhibited by adding 0.7 wt% Zn into SnBi solder paste. In addition, the ultimate tensile strength of SnBi solder increased by 6.05% after soldering. Zhu et al. [9] found that the addition of Al<sub>2</sub>O<sub>3</sub> nanoparticles with a medium concentration could make the Sn-rich and Bi-rich phases in SnBi solder distribute more uniformly. Shen et al. [10] proved that the 0.1 wt% Cu addition had a positive effect on the wetting behaviour of SnBi solder.

Improving the surface finish of the substrate is another effective method to improve the performance of SnBi solder joints. Common substrate surface finish treatment methods include organic solderability preservative (OSP) [11], electroless nickel immersion gold (ENIG) [12] and electroless

nickel immersion palladium gold (ENEPIG) [13]. Zhang *et al.* [14] found that adding Ni element to the surface of the Cu substrate can refine the IMC grain and improved the shear strength of the solder joints. Hu *et al.* [15] and Zou *et al.* [16] added trace amounts of Ag, Al, Sn or Zn elements into Cu substrate and found that the interfacial Bi embrittlement in the SnBi/Cu solder joint was restrained. Meanwhile, the void at the interface was eliminated. The SAC solder coated with a thickness of about 5  $\mu\text{m}$  was obtained on the Cu pad using hot air solder levelling (HASL) by Wang *et al.* [17]. The study found that the SAC coating helped to inhibit the growth of the IMC layer at the interface of the SnBi/Cu solder joint during soldering and isothermal ageing and improved the shear strength and ductility of the SnBi/Cu solder joint.

Our previous results showed that the SnBi/SACBN/Cu composite solder joints with superposition structure can be successfully fabricated and the interface brittleness of SnBi/Cu solder joints is effectively suppressed after reflow soldering. However, the performance changes of the composite solder joints during ageing are still unknown. Therefore, the evolution of the microstructure, shear behaviour and hardness of the SnBi/SACBN/Cu composite solder joint during isothermal ageing were investigated in this study in comparison with the SnBi/Cu and SACBN/Cu solder joints.

## 2. Experimental procedures

The SACBN solder ball and SnBi solder paste were the main solder materials used in this study. The SACBN solder balls were made through cutting and melting processes in glycerol. The SnBi solder paste was a commercial product with eutectic composition. The melting temperature of SACBN and SnBi solder was 220  $^{\circ}\text{C}$  and 139  $^{\circ}\text{C}$  respectively. The customized printed circuit board (PCB) with Cu pads was used as substrate. The diameter of these Cu pads was 640  $\mu\text{m}$ . Firstly, the PCB was cleaned by ethanol under ultrasonic condition for 10 min.

Secondly, the SACBN ball with the diameter of 550  $\mu\text{m}$  were positioned onto the Cu pads with flux and then soldered on a heating platform at 260 $^{\circ}\text{C}$  for 90s. The AMTECH 4300LF washable flux was used during this soldering process. Then the soldered samples were cooled to room temperature and were cleaned by ethanol to remove residual flux. Finally, the SnBi solder paste was dispensed onto the soldered SACBN joints by the Create-PSD solder paste dispenser. The samples were soldered at 160  $^{\circ}\text{C}$  for 90 s to form the solder joints with superposition structure. The schematic diagram of the fabrication process is presented in Figure 1. For comparison purpose, the SACBN/Cu and SnBi/Cu solder joints with the same geometric size were made at 260 $^{\circ}\text{C}$  and 160 $^{\circ}\text{C}$  for 90 s respectively. Here the height of all the three kinds of solder joints is 790  $\mu\text{m}$ .

The solder joints were further aged at 100 $^{\circ}\text{C}$  for 600 h in the thermostatic ageing furnace. The cross-sectional samples of the three solder joints before and after ageing were prepared by grinding and polishing. The evolution of the microstructures during thermal ageing were investigated with the Metallographic microscope. The chemical compositions of the solder joints were analysed with the energy dispersive X-ray and spectrometer (EDS). The shear behaviour of the solder joints was studied with the RESCH PTR-1000 bond tester. The shear height was set as 45  $\mu\text{m}$  and the shear speed was 0.1 mm/s. The fracture morphology was observed with the SEM. Besides, the SHIMADZU DUH-211S hardness tester equipped with a Berkovich indenter was used for the characterizing the microhardness of solder joints. The nanoindentation test was performed in several bulk solders for each kind of joint. At least 10 positions were tested for getting the average hardness. The loading force and holding time of the nanoindentation hardness test was set as 100 mN and 10 s, respectively. The Poisson's ratio of 0.35 was selected for this study. The loading and unloading mode was applied at a rate of 5 mN/s.

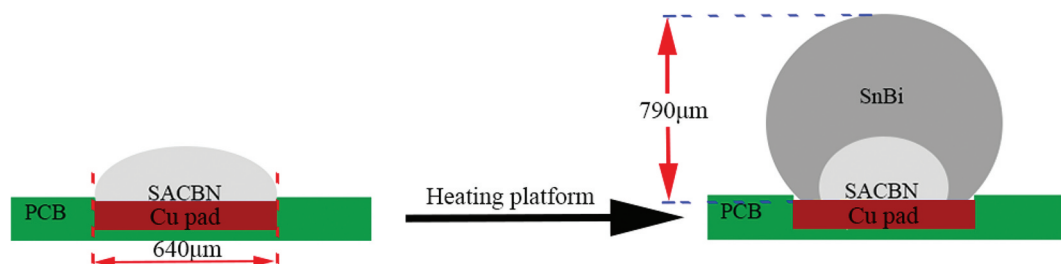


Figure 1. Schematic diagram of the fabrication of the SnBi/SACBN/Cu solder joint.

### 3. Results and discussion

#### 3.1 Microstructure of the solder joints

Figure 2 illustrates the overall structure and the microstructure of the three solder joints. As shown in Figure 2(c), by comparison with the Sn58Bi (SnBi) and Sn0.7Ag0.5Cu3.5Bi0.05Ni (SACBN) solder joint, the overall structure of the SnBi/SACBN/Cu solder joint is composed of two parts. The SnBi eutectic structure is located above the SACBN bulk to form a composite solder joint with an overlapping structure. The Sn dendritic in the SnBi bulk appears clear sunlight morphology along with the SACBN bulk as marked by the red line and arrows, which correspond to the Sn dendrites in SnBi bulk. It can be deduced that the Sn grains in the SACBN bulk affect the formation and growth of the Sn dendritic in the SnBi bulk. Figure 2(a) displays that the SnBi/Cu solder joints consist of dense Sn phases and Bi-rich phases. This dense microstructure is consistent with the previous studies [18]. As shown in Figure 2(b), the SACBN/Cu solder joint consists of a large amount of Sn and dense eutectic structures. Compared Figure 2(a)

with Figure 2(c), the number of Sn phases increases significantly and the number of Bi-rich phases decreases. Since the concentration of Sn in the SACBN bulk is higher than that in the SnBi alloy, Sn atoms diffuse from the SACBN bulk into the molten SnBi solder during the second soldering step. Therefore, the concentration of Sn in the SnBi bulk increases, which results in the formation of large Sn grain.

Figure 3 shows the microstructures of the three solder joints under isothermal ageing for 0 h and 600 h at 100°C. Compared with the joint aged for 0 h in Figure 3(a), the size of the Bi-rich phase grains in the SnBi/Cu solder joint aged at 600 h in Figure 3(e) has an increasing trend. However, the number of Bi-rich phases with a smaller size reduces. Similar phenomenon is also found in the comparison of the microstructure of the composite solder joints before and after ageing, as shown in Figure 3(c and g). This phenomenon can be attributed to the Ostwald ripening of Bi element during the isothermal ageing. In addition, the eutectic structure of the SACBN/Cu solder joint significantly increases after ageing for 600 hours, as

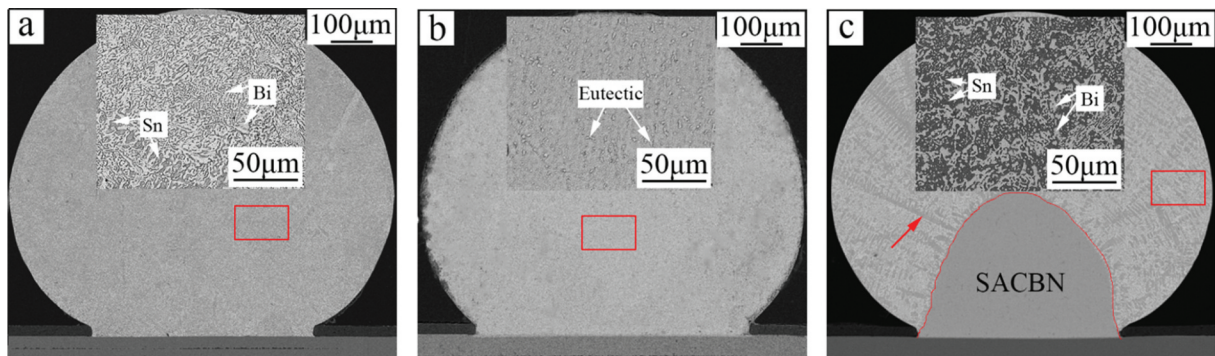


Figure 2. Overall structure and microstructure of the solder joints. (a) SnBi/Cu, (b) SACBN/Cu, (c) SnBi/SACBN/Cu.

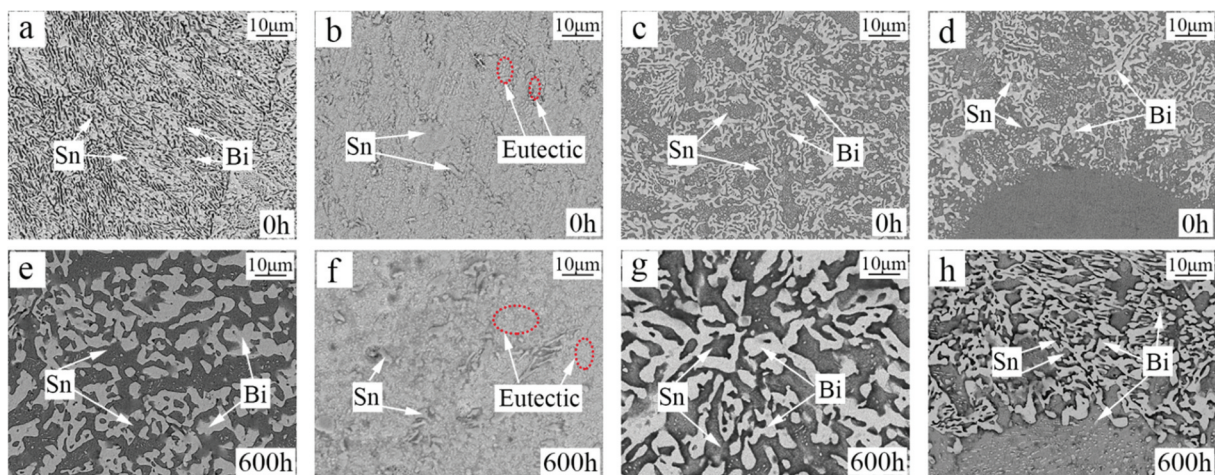


Figure 3. SEM micrographs of the solder bulks before and after isothermal ageing. (a) and (e) SnBi/Cu, (b) and (f) SACBN/Cu, (c) and (g) SnBi bulk in SnBi/SACBN/Cu, (d) and (h) SnBi/SACBN interface in SnBi/SACBN/Cu.

shown in Figure 3(f). The microstructure in Figure 3(h) indicates that the Sn at the interface of SnBi/SACBN still radially distributes after ageing. Many Bi phases can be observed in the SACBN area, which is caused by element diffusion during the isothermal ageing process.

Figure 4 shows the mapping of various elements on the SnBi/SACBN interface after isothermal ageing for 600 hours. As shown in Figure 4(b), the Sn element continuously distributes on the SnBi/SACBN interface. It can be deduced that the microstructure of the SACBN region has an effect on the formation and growth of the Sn phase in the SnBi region during the second soldering process of the composite solder joint. The structure in Figure 2(c) also confirms the above phenomenon. It is suggested that the solid-liquid diffusion between the two solders during the second soldering process and the solid-solid diffusion during the isothermal ageing process are the main reasons for the distribution of a large amount of Bi element in the SACBN region of the composite solder joint, as shown in Figure 4(c). In addition, Figure 4(d,e and f) illustrate that the elements of Ag, Cu and Ni evenly distributes in SnBi/SACBN.

Figure 5 shows the interfacial microstructures and EDS analysis of the three solder joints before and after isothermal ageing at 100°C. It can be observed from the figure that the structure of the three solder joints is significantly coarsened after ageing for 600 h. It is well known that  $\text{Cu}_6\text{Sn}_5$  is

the main phase produced by the SnBi solder soldered on the Cu substrate [19], which is also consistent with the EDS analysis in Figure 5(g). Compared Figure 5(a) with Figure 5(d), the thickness of interfacial IMC significantly increases. This phenomenon can be attributed to the solid-solid diffusion that occurs at the solder joint interface during high temperature ageing. On the other hand, the annexation and merging of adjacent grains in the IMC is an important reason for the increase of the thickness of the interfacial IMC after ageing. As shown in Figure 5(b), the interfacial IMC in SACBN/Cu joint is  $(\text{Cu}, \text{Ni})_6\text{Sn}_5$ . Compared Figure 5(b) with Figure 5(e), the IMC shows a tendency to diffuse into the SACBN bulk solder. Due to the addition of the SACBN bump, the interfacial reaction in the composite joint is between SACBN and Cu. Therefore, the IMC on the interface of SnBi/SACBN/Cu joint is  $(\text{Cu}, \text{Ni})_6\text{Sn}_5$ , as shown in Figure 5(c). Compared Figure 5(c) with Figure 5(f), the thickness of and grain size of the interfacial IMC  $(\text{Cu}, \text{Ni})_6\text{Sn}_5$  increase significantly. Meanwhile, a small amount of the interfacial IMC diffuses into the bulk solder during ageing. It can be seen that the thickness of the interfacial IMC in the SnBi/Cu solder joint is the thinnest among the three kinds of solder joints. This is due to the formation of a large amount of Bi-rich grains above the  $\text{Cu}_6\text{Sn}_5$  IMC layer on the substrate. Therefore, the growth of the IMC layer is suppressed and the thin and flat state is exhibited.

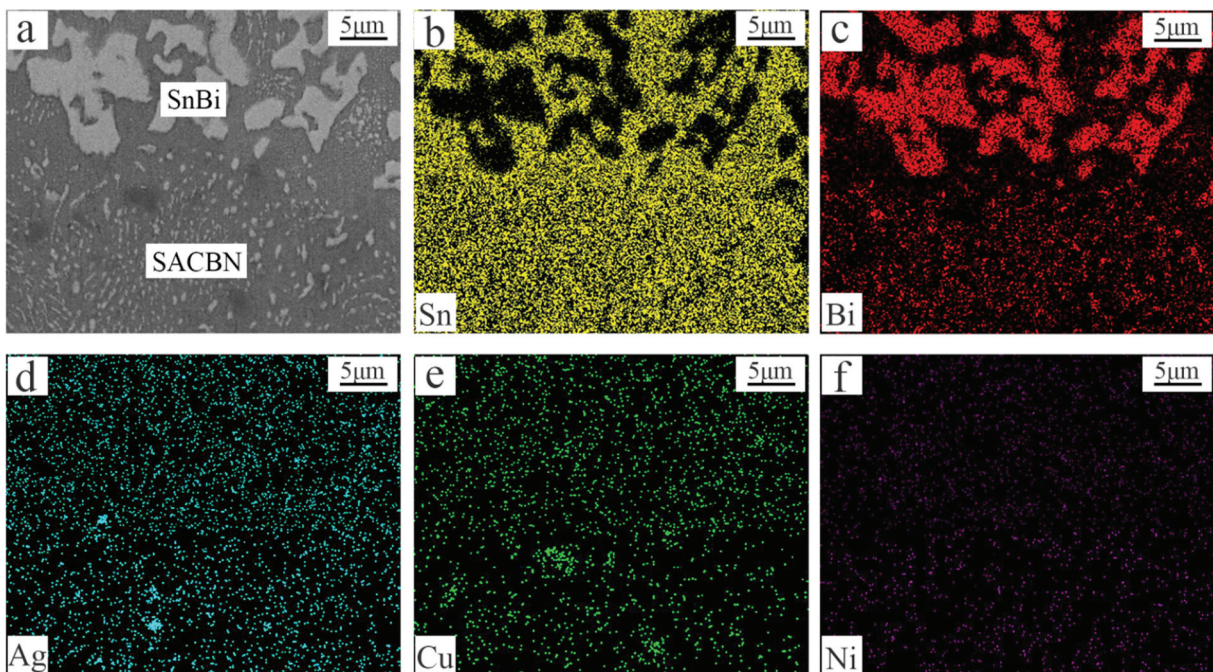
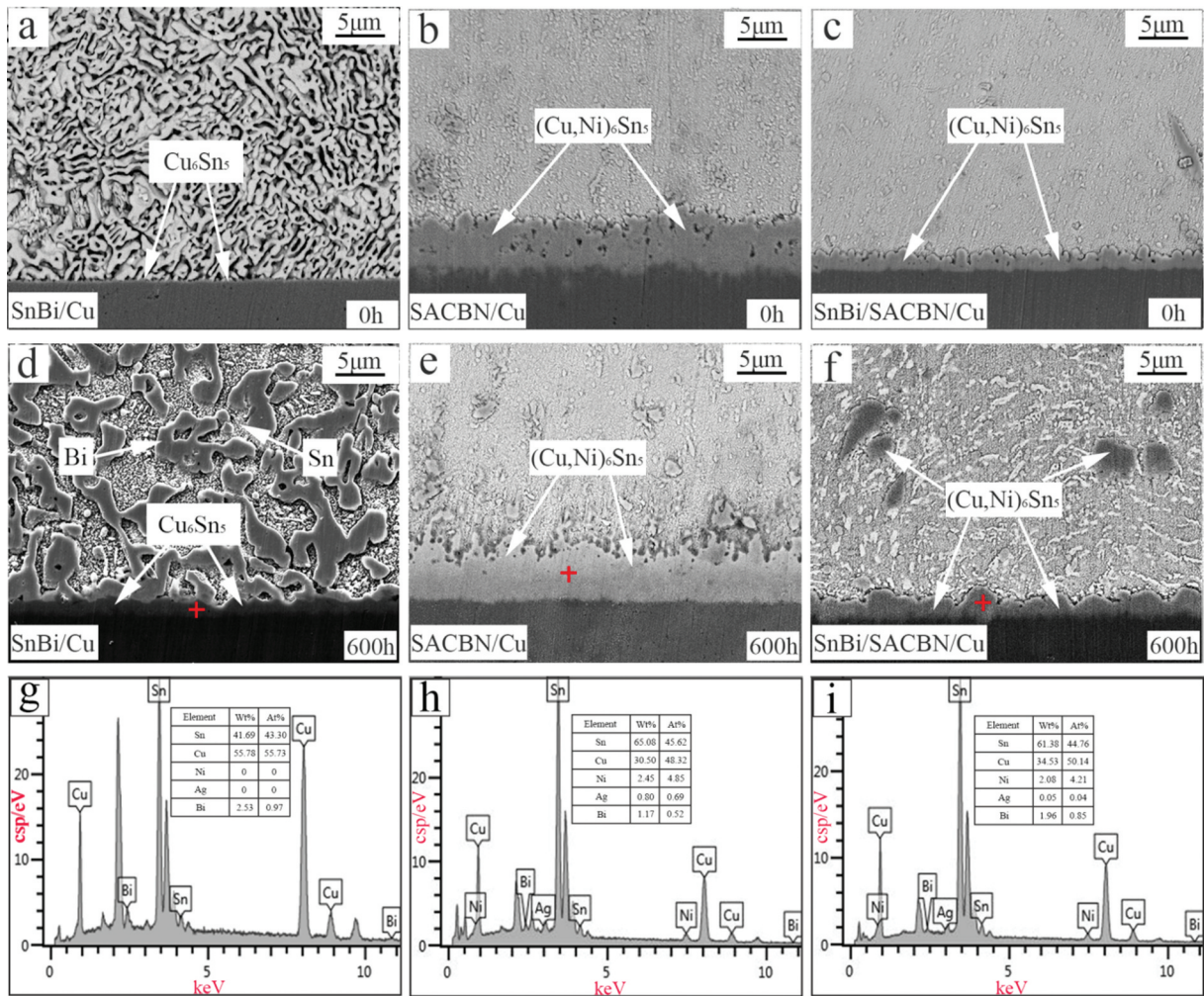


Figure 4. SEM and element mapping of the SnBi/SACBN interface after ageing. (a) Microstructure, (b) Sn element mapping, (c) Bi element mapping, (d) Ag element mapping, (e) Cu element mapping, (f) Ni element mapping.



**Figure 5.** SEM morphology and EDS analysis of the IMC layers in the solder joints before and after ageing. (a) and (d) SnBi/Cu, (b) and (e) SACBN/Cu, (c) and (f) SnBi/SACBN/Cu, (g) EDS of the point in (d), (h) EDS of the point in (e), (i) EDS of the point in (f).

### 3.2 Mechanical Properties of the solder joints

Figure 6 shows the average shear strength of the three solder joints before and after isothermal

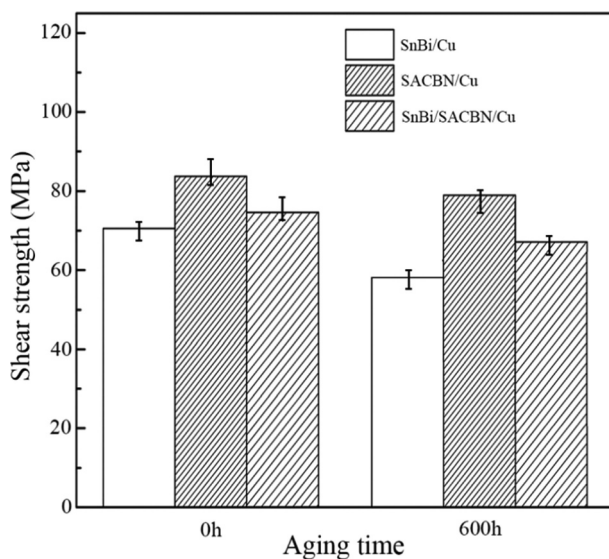


**Figure 6.** The average shear strength of the three kinds of the solder joints before and after ageing.

ageing. The average shear strength of the SnBi/Cu solder joint is 68.2 MPa, which is much lower than that of the other two joints. That is caused by the presence of a great deal of hard and brittle Bi-rich phases in the SnBi/Cu interface and the thin IMC, as shown in Figure 5(a). Among these three solder joints, the SACBN joint achieves the highest shear strength of 85.2 MPa. The strength of the SnBi/SACBN/Cu composite solder joint is 74.4 MPa, which is higher than that of the SnBi/Cu solder joints. The average shear strength of the three solder joints all reduce after isothermal ageing for 600 h. The coarsening of the structure of the solder joint during the ageing process is considered as the main reason for the decrease of the shear strength, which also proves that the ageing process can weaken the barrier effect of the SACBN barrier layer. However, the shear strength of SnBi/SACBN/Cu is always higher than that of SnBi/Cu.

Figure 7 shows the shear curves of the three solder joints before and after isothermal ageing. The shear strength of the SnBi/Cu solder joints

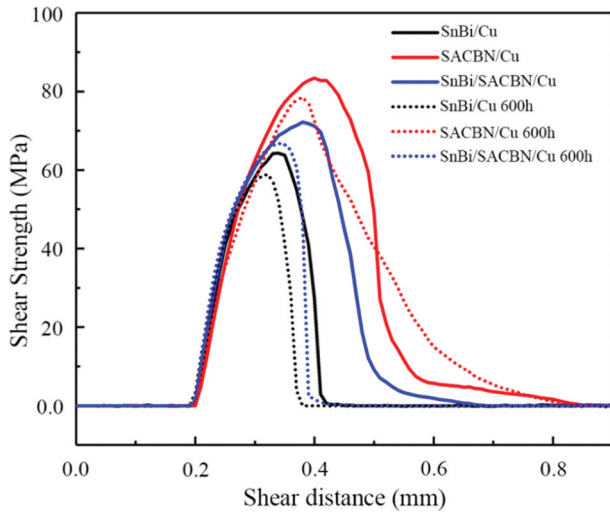


**Figure 7.** Shear strength-distance relationships of the three solder joints before and after isothermal ageing.

drops after reaching the peak, which indicates that brittle fracture occurs in the SnBi/Cu solder joints before isothermal ageing. The shear force of SACBN/Cu increases to the maximum at first and then decreases slowly during the shear test. According to the study by Di Maio and Hunt [20], Sn is ductile phase. Therefore, the solder joint

demonstrates clear ductile failure behaviour. The shear curve of the SnBi/SACBN/Cu composite solder joints is similar to that of the SACBN/Cu joints. Obviously, the SACBN bumps in the composite joint act as a barrier layer, which suppresses the brittleness of the SnBi solder joint. The failure mode of SnBi/SACBN/Cu is suggested to be brittle-ductile failure before ageing. As shown in Figure 7, the SnBi/Cu and SACBN/Cu joints after isothermal ageing show similar failure modes with that before ageing. However, the shear curve of the composite solder joint after ageing is similar to SnBi/Cu and the failure mode shifts from brittle-ductile failure to brittle failure.

As shown in Figure 8(a and d), the SnBi/Cu fracture surface shows smooth and bright morphology. Therefore, clear brittle fracture occurs near the substrate in the SnBi/Cu solder joints before and after ageing due to the high concentration of the hard and brittle Bi-rich phases. In contrast, the fracture morphology of the SACBN/Cu joint shows a large number of dimples, as shown in Figure 8(b and e). Therefore, plastic fracture occurs in the SACBN/Cu solder joints before and after

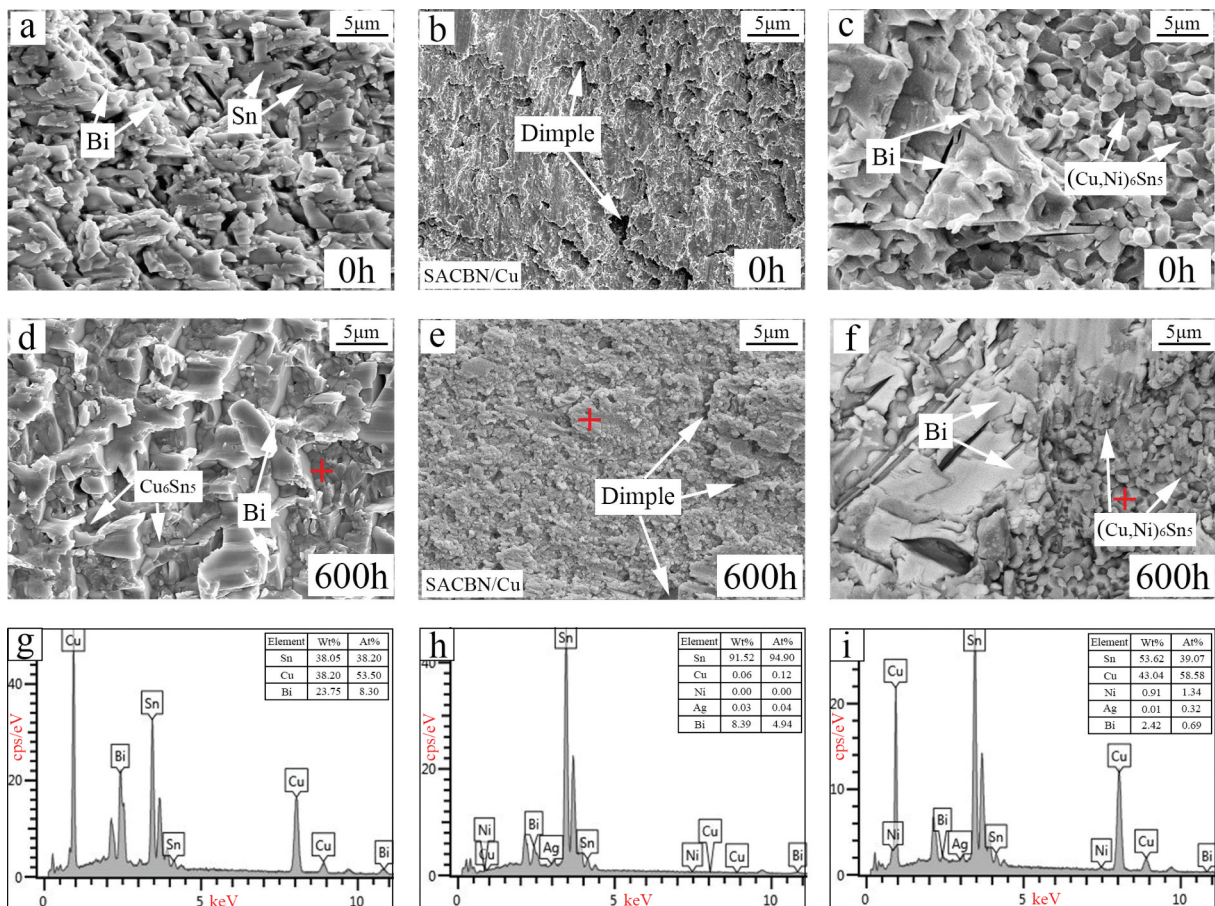


**Figure 8.** Shear morphology and EDS analysis of the three solder joints before and after ageing. (a) as-soldered SnBi/Cu, (b) as-soldered SACBN/Cu, (c) as-soldered SnBi/SACBN/Cu, (d) SnBi/Cu after ageing, (e) SACBN/Cu after ageing, (f) SnBi/SACBN/Cu after ageing, (g) EDS of the point in (d), (h) EDS of the point in (e), (i) EDS of the point in (f).

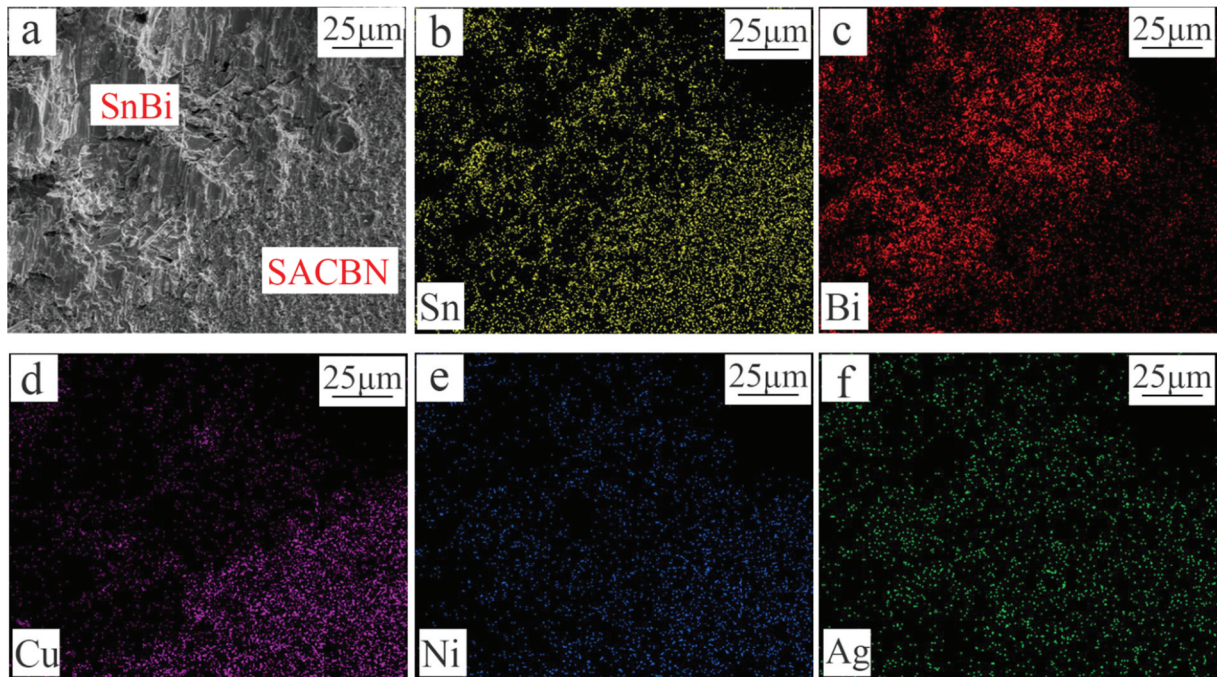


**Figure 9.** SEM and elemental mapping of the SnBi/SACBN/Cu joint aged at 100°C for 600 h. (a) microstructure, (b) element mapping of Sn, (c) element mapping of Bi, (d) element mapping of Cu, (e) element mapping of Ni. (f) element mapping of Ag.

ageing. The results of [Figure 8\(i\)](#) and [Figure 9](#) show that the SnBi/SACBN/Cu failures appear in both the SnBi bulk and SACBN/Cu interface after ageing.

[Figure 10](#) is the top view of the fractured SnBi/SACBN/Cu composite solder joints before and after ageing. An interesting phenomenon can be observed from the figure. The area of SACBN in the fracture section without ageing is very large, while the area of SACBN reduces significantly after ageing for 600 hours. In [Figure 11\(d and f\)](#), Ag and Ni diffuse evenly to the entire pad. The reason for this phenomenon is that the elements in SACBN area diffuse into SnBi alloy by solid-

solid diffusion during the isothermal ageing. Therefore, the content of SACBN in the composite solder joint after ageing reduces. As shown in [Figure 11\(b and e\)](#), the fracture section of the SACBN area is mainly composed of Sn and Cu. As shown in [Figure 11\(c\)](#), the fracture section of the SnBi area is composed of a large amount of Bi. This phenomenon once again proves that the SACBN area in the composite solder joint fractures at the interface and the SnBi area fractures in the bulk solder.

In order to eliminate the influence of the loading position of the load on the bulk solder on the

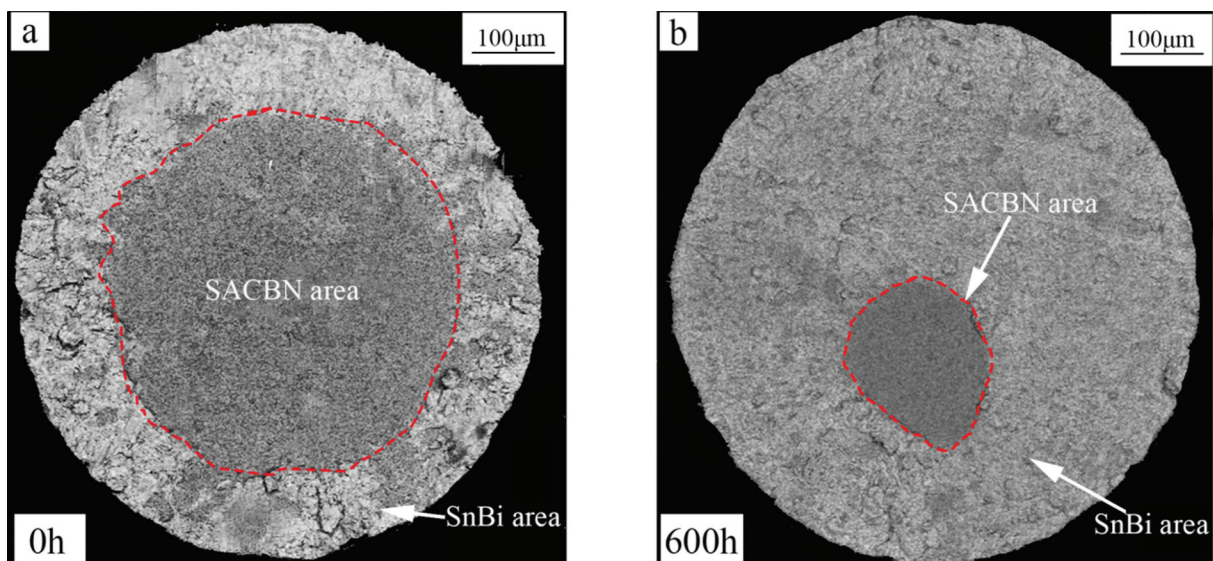


**Figure 10.** Shear fractures of SnBi/SACBN/Cu. (a) top view of as-soldered joint, (b) top view of aged joint.

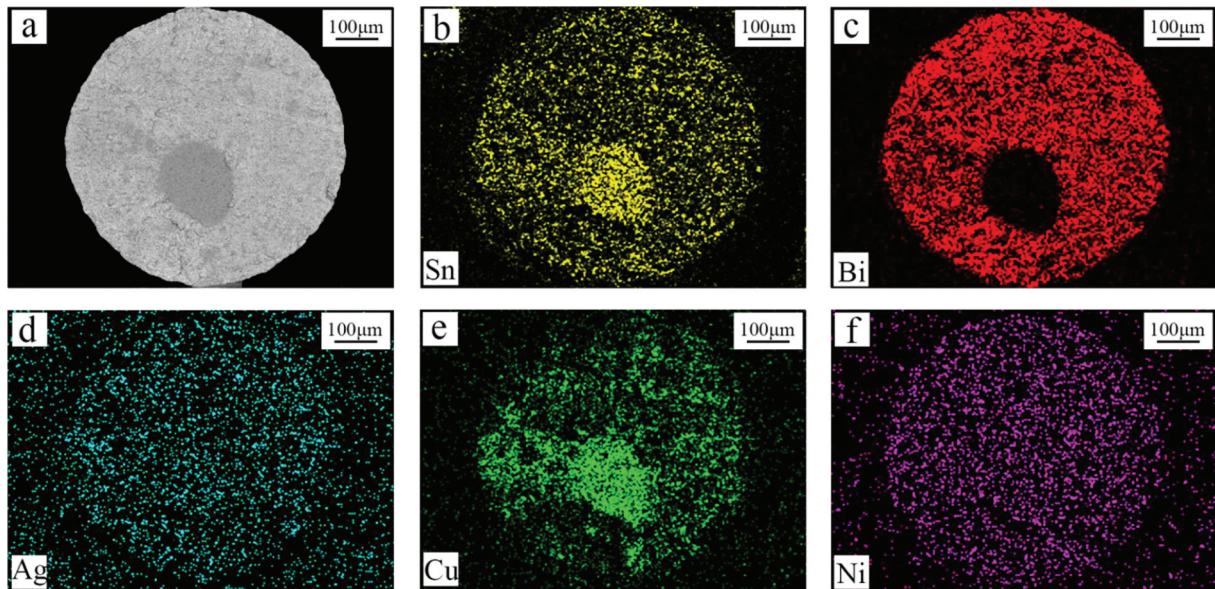


**Figure 11.** Element mapping of the shear fracture of SnBi/SACBN/Cu joint aged at 100°C for 600 h. (a) microstructure, (b) element mapping of Sn, (c) element mapping of Bi, (d) element mapping of Cu, (e) element mapping of Ni. (f) element mapping of Ag.

hardness value of the bulk solder. In the nanoindentation hardness test, the loading positions of the bulk solder with the same solder joints are also similar and each area is subjected to 10 loading experiments. To get the average hardness of the bulk solder. The maximum load of the nanoindentation hardness test is 100 mN, the maximum load holding time is 10 s, the Poisson's ratio is 0.35, and the loading and unloading rates are both 5 mN/s. The comparison of the average hardness of the three solder joints before and after ageing is shown in Figure 12. The average hardness of the SnBi/Cu solder joint is 304.7MPa, which is much higher

than that of the other two. The hardness of the SACBN/Cu bulk solder is the lowest due to its high concentration of soft  $\beta$ -Sn phase and eutectic structure. The two areas were tested respectively. The average hardness of the SnBi area in the SnBi/SACBN/Cu composite solder joints is 287.5MPa, which is lower than that of the SnBi/Cu solder joints. The Sn element in the SACBN bulk diffuses into the SnBi alloy during the second soldering step and then more  $\beta$ -Sn phases form, which is the main reason for the decrease of hardness in the SnBi region. The average hardness of SACBN area in the composite solder joints is higher than that of

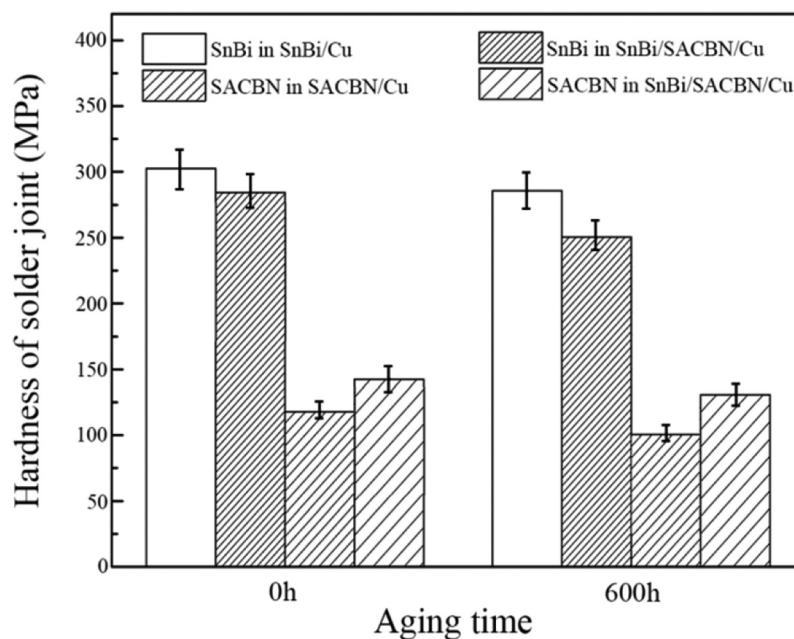


**Figure 12.** Hardness of the solder bulks.

SACBN/Cu. The diffusion of Bi atoms from the SnBi area into the SACBN area results in a strengthening effect and leads to the increase of hardness. After ageing at 100°C for 600 h, the average hardness of the three solder joints has a decreasing tendency, which can be attributed to the coarsening of the microstructure. Thus, the addition of SACBN bulk to the SnBi/Cu joints will significantly reduce the average hardness of SnBi alloys before and after ageing.

#### 4. Conclusions

- (1) The addition of the SACBN layer increases the concentration  $\beta$ -Sn phase in the SnBi/Cu solder joint.
- (2) The addition of SACBN bulk suppresses the brittle fracture of SnBi/Cu and the failure mode changes from brittle fracture to brittle-ductile hybrid fracture during the shear test.
- (3) The massive diffusion of elements leads to a reduction in the relative area of the SACBN region during the ageing process.
- (4) The addition of SACBN bulk into the SnBi/Cu joint significantly reduce the average hardness of SnBi alloy before and after ageing.

#### Disclosure Statement

No potential conflict of interest was reported by the author(s).

#### ORCID

Yang Liu  <http://orcid.org/0000-0002-4311-2198>

#### References

- [1] Yang L, Zhou W, Ma Y, et al. Effects of Ni addition on mechanical properties of Sn58Bi solder alloy during solid-state aging. *Mater Sci Eng A*. 2016;667:368–375.
- [2] Lai Z, Ye D. Microstructure and fracture behavior of non eutectic Sn-Bi solder alloys. *J Mater Sci Mater Electron*. 2016;27:3182–3192.
- [3] Ye D, Du C, Wu M, et al. Microstructure and mechanical properties of Sn-xBi solder alloy. *J Mater Sci Mater Electron*. 2015;26:3629–3637.
- [4] Lai Z, Ye D. Microstructure and properties of Sn-10Bi-xCu solder alloy/joint. *J Electron Mater*. 2016;45:3702–3711.
- [5] Cheng J, Hu X, Li Q, et al. Influences of Ni addition into Cu-x Ni alloy on the microstructure evolution and mechanical property of Sn-58Bi/Cu-x Ni solder joint. *Appl Phys A*. 2020;126:1–10.
- [6] Zhou S, Yang C, Lin S, et al. Effects of Ti addition on the microstructure, mechanical properties and electrical resistivity of eutectic Sn58Bi alloy. *Mater Sci Eng A*. 2019;744:560–569.
- [7] Sun H, Chan YC, Wu F. The impact of reflow soldering induced dopant redistribution on the mechanical properties of CNTs doped Sn58Bi solder joints. *J Mater Sci Mater El*. 2015;29:5318–5325.
- [8] Ma D, Wu P. Effects of Zn addition on mechanical properties of eutectic Sn-58Bi solder during liquid-state aging. *Nonferrous Met Soc*. 2015;25:1225–1233. .
- [9] Zhu W, Ma Y, Li X, et al. Effects of Al<sub>2</sub>O<sub>3</sub> nanoparticles and properties of Sn58Bi solder alloys. *J Mater Sci Mater El*. 2018;29:7575–7585.
- [10] Shen J, Pu Y, YIN H, et al. Effects of Cu, Zn On the wettability and shear mechanical properties of Sn-Bi-based lead-free solders. *J Electron Mater*. 2015;44:532–541.
- [11] Lee SM, Yoon JW, Jung SB. Interfacial reaction and mechanical properties between low melting temperature Sn-58Bi solder and various surface finishes during reflow reactions. *J Mater Sci Mater El*. 2015;26:1649–1660.
- [12] Myung WR, Kim Y, Jung SB. Evaluation of the bondability of the epoxy-enhanced Sn-58Bi solder with ENIG and ENEPIG surface finishes. *J Electron Mater*. 2015;44:4637–4645.
- [13] Kim J, Myung WR, Jung SB. Effects of aging treatment on mechanical properties of Sn-58Bi epoxy solder on ENEPIG-surface-finished PCB. *J Electron Mater*. 2016;45:5895–5903.
- [14] Zhang X, Hu X, Jiang X, et al. Effect of Ni addition to the Cu substrate on the interfacial reaction and IMC growth with Sn3.0Ag0.5Cu solder. *Appl Phys A*. 2018;124:315.
- [15] Hu FQ, Zhang QK, Jiang JJ, et al. Influences of Ag addition to Sn-58Bi solder on SnBi/Cu interfacial reaction. *Mater Lett*. 2018;214:142–145.
- [16] Zou HF, Zhang QK, Zhang ZF. Interfacial microstructure and mechanical properties of SnBi/Cu joints by alloying Cu substrate. *Mater Sci Eng A*. 2012;532:167–177.
- [17] Wang F, Li D, Zhang Z, et al. Improvement on interfacial structure and properties of Sn-58Bi/Cu joint using Sn-3.0Ag-0.5Cu solder as barrier. *J Mater Sci Mater El*. 2017;28:19051–19060.
- [18] Xu R, Liu Y, Zhang H, et al. Evolution of the microstructure of Sn58Bi solder paste with Sn-3.0Ag-0.5Cu addition during isothermal aging. *J Electron Mater*. 2019;48:1758–1765.
- [19] Pang XY, Shang PJ, Wang SQ, et al. Weakening of the Cu/Cu<sub>3</sub>Sn(100)Interface by Bi impurities. *J Electron Mater*. 2010;39:1277–1278.
- [20] Maio D, Hunt C. Time-lapse photography of the  $\beta$ -Sn/ $\alpha$ -Sn allotropic transformation. *J Mater Sci Mater El*. 2009;20:386–391.